Neutrino emission in neutron stars

E. N. E. van Dalen*
Theory Group, Kernfysisch Versneller Instituut, University of Groningen, Zernikelaan 25, 9747 AA Groningen, The Netherlands

A. E. L. Dieperink†
Theory Group, Kernfysisch Versneller Instituut, University of Groningen, Zernikelaan 25, 9747 AA Groningen, The Netherlands and ECT, I-38050, Villazzano, Trento, Italy

J. A. Tjon‡
Theory Group, Kernfysisch Versneller Instituut, University of Groningen, Zernikelaan 25, 9747 AA Groningen, The Netherlands and Jefferson Laboratory, Newport News, Virginia 23606

(Received 22 November 2002; published 27 June 2003)

Neutrino emissivities in a neutron star are computed for the neutrino bremsstrahlung process. In the first part, the electroweak nucleon-nucleon bremsstrahlung is calculated in free space in terms of an on-shell T matrix using a generalized low-energy theorem. In the second part, the emissivities are calculated in terms of the hadronic polarization at the two-loop level. Various medium effects, such as finite particle width, Pauli blocking in the T matrix are considered. Compared to the pioneering work of Friman and Maxwell in terms of (antisymmetrized) one-pion exchange, the resulting emissivity is about a factor 4 smaller at saturation density.

DOI: 10.1103/PhysRevC.67.065807 PACS number(s): 13.75.Cs, 26.60.+c, 21.30.−x

I. INTRODUCTION

The cooling of neutron stars proceeds via the weak interaction. Since in general one-body processes are kinematically forbidden, the dominant reactions are assumed to be the neutral current two-particle processes

$$n+n\rightarrow n+n+\nu_f+\overline{\nu}_f, \tag{1}$$

$$n+p\rightarrow n+p+\nu_f+\overline{\nu}_f, \tag{2}$$

and the charged current ''modified URCA'' process

$$N+n\rightarrow N+p+\overline{\nu}_e+e^-. \tag{3}$$

Standard cooling scenarios are mostly based upon the pioneering work of Friman and Maxwell [1]. In essence, their approach amounts to a convolution of the soft free space neutrino pair emission and two-body (modified) URCA processes (1)–(3) with a finite temperature free Fermi-gas model using Fermi's golden rule to obtain the emission rate. In doing so, a number of simplifying assumptions were made; in particular (i) the two-body interaction between the nucleons was approximated by a central Landau interaction plus a one-pion exchange to represent the tensor force, (ii) only the nonrelativistic limit was considered, (iii) since it is based upon the quasiparticle approximation, nonperturbative effects such as the Landau-Pomeranchuk-Migdal (LPM) effect were not taken into account, (iv) other medium effects such as Pauli blocking in the strong interaction were neglected. It is the aim of the present paper to investigate and possibly improve these assumptions.

In the first part we consider reactions (1) and (2) in free space. Using the fact that the energy release in the bremsstrahlung process is very small, we apply the soft bremsstrahlung formalism of Hanhart *et al.* [2] and Timmermans *et al.* [3]. This allows one to express the bremsstrahlung process in the soft limit model independently in terms of an on-shell T matrix, i.e., phase shifts. In this way we are able to judge the accuracy of past bremsstrahlung calculations, which were mostly based upon the use of a one-pion exchange (OPE) approximation in the nonrelativistic limit [1,4]. In the latter case simplifications occur, such as the vanishing of the vector current matrix elements.

In the second part we consider the process (1) in the medium. To describe the cooling process of neutron stars through neutrino emission, the application of Fermi's golden rule in the quasiparticle approximation (QPA) was mostly used in the past. To compute emissivities beyond QPA, one needs to start from quantum transport equations. The essential physics is then contained in the neutrino self-energies, which appear in the loss and gain terms. We will compare the diagrams at the hadron two-loop level. It appears that only in lowest order in the imaginary part of the hadronic self-energies the use of closed diagrams and the application of Fermi's golden rule coincide.

From the generalized low-energy theorem [3,2] it follows that the use of the QPA leads to an infrared divergent amplitude, $1/\omega$. The latter is predicted to be quenched [5] in a medium whenever the mean free path of the nucleons becomes on the order of the formation length of the lepton pair. This is also known as the LPM effect in case of electromagnetic interactions. We study the importance of this effect by including a finite single-particle width (imaginary part of the self-energy) that depends on energy and temperature.

*Email address: vandalen@kvi.nl
†Email address: dieperink@kvi.nl
‡Email address: tjon@jlab.org

In practice, in calculating the collision integral one needs to specify the appropriate diagrams and make assumptions about hadronic interactions. In doing so, one must be careful that symmetries such as gauge invariance of the vector current are not violated. We also estimate the Pauli blocking by replacing the T matrix by an in-medium G matrix. In the work of Sedrakian and Dieperink [6], the neutrino emissivity was computed including the LPM effect, however, in the OPE approximation.

Many properties of superfluid matter such as pairing are still known with large uncertainty. Therefore only non-superfluid matter will be considered. For recent papers about pairing, we refer to Gusakov [7] and Yakovlev *et al.* [8].

Although we will apply the present formalism to neutrino pair emission in neutral weak current processes, it is equally valid for soft electromagnetic bremsstrahlung.

This paper is organized as follows. In Sec. II we discuss electroweak bremsstrahlung in free space; in Sec. III the in-medium process is discussed at the two-loop level. In Sec. IV, results are presented showing the effects of various approximations. In the Appendixes a summary of quantum transport theory and finite temperature Green's functions are presented.

II. ELECTROWEAK BREMSSTRAHLUNG IN FREE SPACE

A. Soft electroweak bremsstrahlung amplitude

The $\nu\overline{\nu}$ pair emission in a neutron star is characterized by a very small energy transfer (on the order of the temperature $T\simeq 1$ MeV), much smaller than any other scale in the process like m_{π} or p_F. Therefore it is natural to consider the $NN\rightarrow NN\nu\overline{\nu}$ process in the ultrasoft limit. For simplicity and also to be consistent with the low density limit of the medium, we will first consider this process in free space.

Here the treatment of soft NN electroweak bremsstrahlung, discussed in more detail in Ref. [3], is summarized. Analogous to the electromagnetic bremsstrahlung (see the work of Low, Ref. [9]), the first two terms of the expansion in powers of the energy-momentum transfer $|\vec{q}|<\omega$ of the electroweak bremsstrahlung amplitude are determined by the amplitude for the corresponding nonradiative process $M=A/\omega+B+O(\omega)$. In the ultrasoft regime ($\omega/p\ll 1$, where p is the nucleon momentum), the B and higher order terms can be neglected. The amplitude of the diagrams in Fig. 1 with radiation from external legs only is given [2,3] by

$$M_{\nu}^{ext,a}=T_1 S(p_1-q)\Gamma_{\nu}^{a}+\Gamma_{\nu}^{a}S(p_1'+q)T_1'+\{1\leftrightarrow 2\}. \quad (4)$$

The A term in the Low expansion is obtained by considering the limit $|\vec{q}|<\omega\rightarrow 0$ of $\omega M_{\nu}^{ext,a}$; to this end we expand the various T's with one nucleon off its mass shell,

$$T_1=\langle p_1',p_2'|T|p_1-q,p_2\rangle,$$

$$T_1'=\langle p_1'+q,p_2'|T|p_1,p_2\rangle, \quad (5)$$

around the on-shell point T_0,

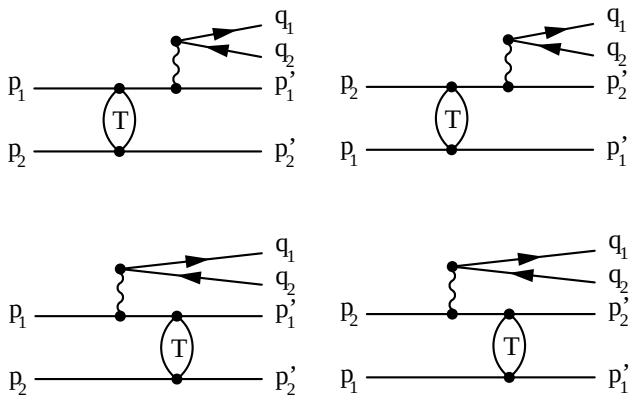

FIG. 1. Diagrams for neutrino pair bremsstrahlung of order $1/\omega$ with radiation from external legs.

$$T_1=T_0-q\cdot\frac{\partial}{\partial p_1}T_0+\cdots,$$

$$T_1'=T_0+q\cdot\frac{\partial}{\partial p_1'}T_0+\cdots, \quad (6)$$

and the nucleon propagator S as

$$S(p\pm q)=\frac{\Lambda^{+}(p)+\Lambda^{-}(p)}{\not p\pm\not q-m}\approx\pm\frac{2m\Lambda^{+}(p)}{2p\cdot q}+O(1) \quad (7)$$

with $\Lambda^{\pm}(p)=(\pm\not p+m)/2m$.

The hadronic weak interaction vertex in the limit $q\rightarrow 0$ is given by

$$\Gamma_{\nu}^{a}=\frac{G_F}{\sqrt{2}}\gamma_{\nu}(c_V-c_A\gamma_5)\frac{\tau_a}{2}, \quad (8)$$

where G_F is the Fermi weak coupling constant and τ is the isospin operator. The vector and axial-vector coupling constants for neutrons are $c_V^n=-1$, $c_A^n=-g_A=-1.26$, and for protons, $c_V^p=1-4\sin^2\Theta_W\approx 0.08$, $c_A^p=g_A=1.26$.

Since the initial/final particles are on mass shell, one has the relations $(\not p+m)\gamma_{\nu}u(p)=2p_{\nu}u(p)$ and $\overline{u}(p)\gamma_{\nu}(\not p+m)=2p_{\nu}\overline{u}(p)$, which are useful for the vector current. As a result, in the ultrasoft region ($q/p\ll 1$) the vector and axial-vector current matrix elements are given by

$$M_{\nu}^{V,a}=\frac{G_F c_V}{2\sqrt{2}}\left(-T_0\frac{p_{1\nu}}{p_1\cdot q}\tau^a+\tau^a\frac{p_{1\nu}'}{p_1'\cdot q}T_0\right)+\{1\leftrightarrow 2\} \quad (9)$$

and

$$M_{\nu}^{A,a}=\frac{2mG_F c_A}{2\sqrt{2}}\left(-T_0\frac{\Lambda^{+}(p_1)}{2p_1\cdot q}\gamma_{\nu}\gamma_5\tau^a+\gamma_{\nu}\gamma_5\tau^a\frac{\Lambda^{+}(p_1')}{2p_1'\cdot q}T_0\right)+\{1\leftrightarrow 2\}, \quad (10)$$

respectively. Naturally, the vector current is conserved: $q^\nu M_\nu^{V,a}=0$.

B. Structure of the elastic *NN* scattering amplitude

It is clear that the amplitudes in Eqs. (9) and (10) depend on the Lorentz structure of T_0. For the elastic NN scattering amplitude [10,11] for the process $N(p_1)+N(p_2)\to N(p_1')+N(p_2')$, the covariant form of the on-shell T matrix can be expressed as

$$\begin{aligned} T&=T^{dir}+T^{exch}\\ &=\sum_{I=0,1}\sum_{\alpha=1}^{5}F_\alpha^{(I)}(s,t,u)[\overline{u}(p_2')\Omega_\alpha u(p_2)\overline{u}(p_1')\Omega^\alpha u(p_1)\\ &\quad+(-)^\alpha\overline{u}(p_1')\Omega_\alpha u(p_2)\overline{u}(p_2')\Omega^\alpha u(p_1)]B_I, \end{aligned} \tag{11}$$

where the five Fermi covariants are

$$\Omega_\alpha=(\Omega_1,\Omega_2,\Omega_3,\Omega_4,\Omega_5)=(1,\sigma_{\mu\nu}/\sqrt{2},\gamma_5\gamma_\nu,\gamma_\nu,\gamma_5). \tag{12}$$

The projection operators on isosinglet and isotriplet states are

$$\begin{aligned} B_0&=(1-\vec{\tau}_1\cdot\vec{\tau}_2)/4,\\ B_1&=(3+\vec{\tau}_1\cdot\vec{\tau}_2)/4, \end{aligned} \tag{13}$$

respectively. $F_\alpha^{(I)}(s,t,u)$ are the invariant functions of the Mandelstam variables $s=-(p_1+p_2)^2$, $t=-(p_1'-p_1)^2$, and $u=-(p_2'-p_1)^2$. For the $nn\nu\overline{\nu}$ and $np\nu\overline{\nu}$ processes the isospin combinations needed are

$$\begin{aligned} F_\alpha^{(nn)}(s,t,u)&=F_\alpha^{(pp)}(s,t,u)=F_\alpha^{(1)}(s,t,u),\\ F_\alpha^{(np)}(s,t,u)&=[F_\alpha^{(1)}(s,t,u)+F_\alpha^{(0)}(s,t,u)]/2, \end{aligned} \tag{14}$$

for $\alpha=1,\ldots,5$. For later use, it is convenient to put the spinors in the exchange term in the "normal order" by introducing the functions

$$T_\alpha^{(I)}(s,t,u)=F_\alpha^{(I)}(s,t,u)+\sum_{\beta=1}^{5}(-1)^\beta C_{\alpha\beta}F_\beta^I(s,t,u), \tag{15}$$

where $C_{\alpha\beta}$ are elements of the Fierz transformation, the explicit form is given [10,11]. Then Eq. (11) can be rewritten as

$$T=\sum_{I=0,1}\sum_{\alpha=1}^{5}T_\alpha^{(I)}(s,t,u)\overline{u}(p_2')\Omega_\alpha u(p_2)\overline{u}(p_1')\Omega^\alpha u(p_1)B_I. \tag{16}$$

Since for a comparison we will need the cross section in the nonrelativistic limit, we also give the required nonrelativistic decomposition of T (we will reserve latin indices for the nonrelativistic T matrix),

$$T=\sum_{\upsilon=1}^{5}\mathcal{T}_\upsilon(s,t,u)O_\upsilon, \tag{17}$$

where

$$\mathcal{T}_\upsilon\equiv(\mathcal{T}_1,\mathcal{T}_2,\mathcal{T}_3,\mathcal{T}_4,\mathcal{T}_5)\equiv(T_C,T_Q,T_{T1},T_{T2},T_{SO}), \tag{18}$$

and the five independent two-body operators

$$O_\upsilon\equiv(1,\vec{\sigma}_1\cdot\vec{n}\vec{\sigma}_2\cdot\vec{n},\vec{\sigma}_1\cdot\vec{k}\vec{\sigma}_2\cdot\vec{k},\vec{\sigma}_1\cdot\vec{k}'\vec{\sigma}_2\cdot\vec{k}',\vec{\sigma}_1\cdot\vec{n}+\vec{\sigma}_2\cdot\vec{n}), \tag{19}$$

with $\hat{k}=(\vec{p}_1'-\vec{p}_1)/|\vec{p}_1'-\vec{p}_1|$, $\hat{k}'=(\vec{p}_1'+\vec{p}_1)/|\vec{p}_1'+\vec{p}_1|$, and $\hat{n}=(\vec{k}'\times\vec{k})/|\vec{k}'\times\vec{k}|$ in the center of mass (c.m.) system. The terms T_C, T_Q, T_{T1}, and T_{SO} correspond to the central, quadratic spin-orbit, tensor, and spin-orbit force, respectively; T_{T2} stands for a second type tensor force (obtained by replacing k by k').

C. The $nn\nu\overline{\nu}$ process

We first treat the $n+n\to n+n+\nu+\overline{\nu}$ process. The vector current amplitude follows from Eq. (9),

$$\begin{aligned} M_\nu^V&=\frac{G_F c_V^n}{2\sqrt{2}}\left(-\frac{p_{1\nu}}{p_1\cdot q}+\frac{p_{1\nu}'}{p_1'\cdot q}-\frac{p_{2\nu}}{p_2\cdot q}+\frac{p_{2\nu}'}{p_2'\cdot q}\right)\\ &\quad\times\sum_{\alpha=1}^{5}F_\alpha^{(nn)}[\overline{u}(p_2')\Omega_\alpha u(p_2)\overline{u}(p_1')\Omega^\alpha u(p_1)\\ &\quad+(-)^\alpha\{p_2'\leftrightarrow p_1'\}]. \end{aligned} \tag{20}$$

The axial-vector current amplitude follows from Eq. (10),

$$\begin{aligned} M_\nu^A&=\frac{2mG_F g_A}{2\sqrt{2}}\sum_{\alpha=1}^{5}F_\alpha^{(nn)}\Bigg[\overline{u}(p_2')\Omega_\alpha u(p_2)\overline{u}(p_1')\\ &\quad\times\left(-\Omega_\alpha\frac{\Lambda^+(p_1)}{2p_1\cdot q}\gamma_\nu\gamma_5+\gamma_\nu\gamma_5\frac{\Lambda^+(p_1)}{2p_1'\cdot q}\Omega^\alpha\right)u(p_1)\\ &\quad+(-)^\alpha\overline{u}(p_1')\Omega_\alpha u(p_2)\overline{u}(p_2')\Bigg(-\Omega_\alpha\frac{\Lambda^+(p_1)}{2p_1\cdot q}\gamma_\nu\gamma_5\\ &\quad+\gamma_\nu\gamma_5\frac{\Lambda^+(p_2')}{2p_2'\cdot q}\Omega^\alpha\Bigg)u(p_1)\Bigg]+(1\leftrightarrow2). \end{aligned} \tag{21}$$

For later use we also give the nonrelativistic limit and the first relativistic correction for the $nn\nu\overline{\nu}$ process by expanding the propagator in terms of $|\vec{p}|/m$,

$$\frac{1}{pq}=\frac{1}{m\omega}\left[1+\frac{\vec{p}\cdot\vec{q}}{m\omega}+O\left(\frac{|\vec{p}|^2}{m^2}\right)\right]. \tag{22}$$

Application to the vector current amplitude yields

$$M_\nu^V=M_\nu^{V,NR}+\Delta M_\nu^V+O(|\vec{p}|^3/m^3), \tag{23}$$

where the nonrelativistic amplitudes $M_\nu^{V,NR}$ vanish and the leading corrections are given by

$$\Delta\vec{M}^V=\frac{G_F c_V^n}{2\sqrt{2}\omega^2 m^2}[\vec{p}_1(\vec{p}_1\cdot\vec{q})-\vec{p}_1'(\vec{p}_1'\cdot\vec{q})+\{1\leftrightarrow 2\}]T^{nn}, \tag{24}$$

$$\Delta M_0^V=\frac{\vec{q}\cdot\Delta\vec{M}^V}{\omega}, \tag{25}$$

with T^{nn} the nonrelativistic reduction of the $I=1$ part of the T matrix in Eq. (11). The vanishing of the nonrelativistic vector amplitude generalizes the result of Friman and Maxwell [1], where this cancellation was observed for Landau-type interaction and OPE, to the complete nn T matrix. This result is, in fact, analogous to the absence of electric-dipole radiation in photon bremsstrahlung processes when the center of mass coincides with the center of charge of the radiating system, e.g., in pp bremsstrahlung.

For the axial-vector current amplitude, one obtains

$$M_\nu^A=M_\nu^{A,NR}+\Delta M_\nu^A+O(|\vec{p}|^2/m^2), \tag{26}$$

where the nonrelativistic amplitudes are given by

$$\vec{M}^{A,NR}=\frac{G_F g_A}{2\sqrt{2}\omega}[T^{nn},\vec{S}]; \quad M_0^{A,NR}=0, \tag{27}$$

and the leading relativistic corrections are

$$\Delta\vec{M}^A=\frac{G_F g_A}{2\sqrt{2}m\omega^2}[T^{nn}\vec{\sigma}_1(\vec{p}_1\cdot\vec{q})-\vec{\sigma}_1 T^{nn}(\vec{p}_1'\cdot\vec{q})+\{1\leftrightarrow 2\}], \tag{28}$$

$$\Delta M_0^A=\frac{G_F g_A}{2\sqrt{2}m\omega}[T^{nn}(\vec{\sigma}_1\cdot\vec{p}_1)-(\vec{\sigma}_1\cdot\vec{p}_1')T^{nn}+\{1\leftrightarrow 2\}], \tag{29}$$

with $\vec{S}=\vec{s}_1+\vec{s}_2$ the total spin of the nn system. Equation (27) has also been derived by Hanhart *et al.* [2] and Timmermans *et al.* [3]. One sees from Eq. (27) that in the nonrelativistic limit there is no contribution from the central interaction T_C, but the axial-vector current amplitude receives contributions from all other terms.

The $pp\nu\bar{\nu}$ process can be treated analogously to the $nn\nu\bar{\nu}$ process. The only differences are the coupling strength to the neutral weak current and the Coulomb corrections in the coefficients $F_\alpha^{(1)}$ of the T matrix.

D. The $np\nu\bar{\nu}$ process

In the $n+p\to n+p+\nu+\bar{\nu}$ process the momenta will be denoted by n and n' (p and p'), for the neutron (proton) in the initial and final states, respectively. In the ultrasoft region ($\omega/p\ll 1$) the vector current amplitude follows from Eq. (9),

$$M_\nu^V=\frac{G_F}{2\sqrt{2}}\left[c_V^n\left(-\frac{n_\nu}{n\cdot q}+\frac{n_\nu'}{n'\cdot q}\right)+c_V^p\left(-\frac{p_\nu}{p\cdot q}+\frac{p_\nu'}{p'\cdot q}\right)\right]\times\sum_{\alpha=1}^{5}F_\alpha^{(np)}[\bar{u}(p')\Omega_\alpha u(p)\bar{u}(n')\Omega^\alpha u(n)+(-)^\alpha\{p'\leftrightarrow n'\}], \tag{30}$$

and the axial-vector current amplitude from Eq. (10),

$$\begin{aligned}M_\nu^A&=M_\nu^{A,dir}+M_\nu^{A,exch}\\&=-\frac{2mG_F g_A}{2\sqrt{2}}\left\{\sum_{\alpha=1}^{5}F_\alpha^{(np)}\left[\bar{u}(p')\Omega_\alpha u(p)\bar{u}(n')\times\left(\Omega_\alpha\frac{\Lambda^+(n)}{2n\cdot q}\gamma_\nu\gamma_5-\gamma_\nu\gamma_5\frac{\Lambda^+(n')}{2n'\cdot q}\Omega^\alpha\right)u(n)-\{(n,n')\leftrightarrow(p,p')\}\right]+(-)^\alpha F_\alpha^{(np)}\right.\\&\left.\times\left[\bar{u}(n')\Omega_\alpha u(p)\bar{u}(p')\left(\Omega_\alpha\frac{\Lambda^+(n)}{2n\cdot q}\gamma_\nu\gamma_5+\gamma_\nu\gamma_5\frac{\Lambda^+(p')}{2p'\cdot q}\Omega^\alpha\right)u(n)-\{(n,n')\leftrightarrow(p,p')\}\right]\right\}.\end{aligned} \tag{31}$$

The exchange terms of the axial-vector current matrix element are included explicitly in Eq. (31). The direct part is analogous to the expression in Eq. (21) for the $nn\nu\bar{\nu}$ process. The only difference is the appearance of a minus sign in the term, where the neutron and proton momenta are interchanged. This is a consequence of the sign difference of the axial-vector coupling constants for neutrons and protons.

The different structure of the exchange part (as compared to the $nn\nu\bar{\nu}$ process) comes from the sign difference between $c_A^{(p)}$ and $c_A^{(n)}$.

Expressions (30) and (31) simplify considerably, if one takes the nonrelativistic limit. Using Eq. (22) one obtains for the vector current amplitude from Eq. (30),

$$\vec{M}^V=-\frac{G_F}{\sqrt{2}}\frac{c_V^n-c_V^p}{2\omega}\frac{\vec{k}}{m}T^{np}, \quad M_0^V=\left(\frac{\vec{q}}{\omega}\right)\cdot\vec{M}^V, \tag{32}$$

and for the axial-vector amplitude from Eq. (31),

$$\vec{M}^A=\frac{G_F g_A}{2\sqrt{2}\omega}([T^{np,dir},\vec{D}]+P_\sigma\{T^{np,exch},\vec{D}\}), \quad M_0^A=0, \tag{33}$$

where $\vec{k}=\vec{n}'-\vec{n}=\vec{p}-\vec{p}'$, $\vec{D}=(\vec{\sigma}_1-\vec{\sigma}_2)$, the spin exchange operator is $P_\sigma=(1+\vec{\sigma}_1\cdot\vec{\sigma}_2)/2$, $\{\ldots,\ldots\}$ denotes the anticommutator, and $T^{np,dir}$ and $T^{np,exch}$ are given by the nonrelativistic reduction of the direct and exchange parts of the np T matrix.

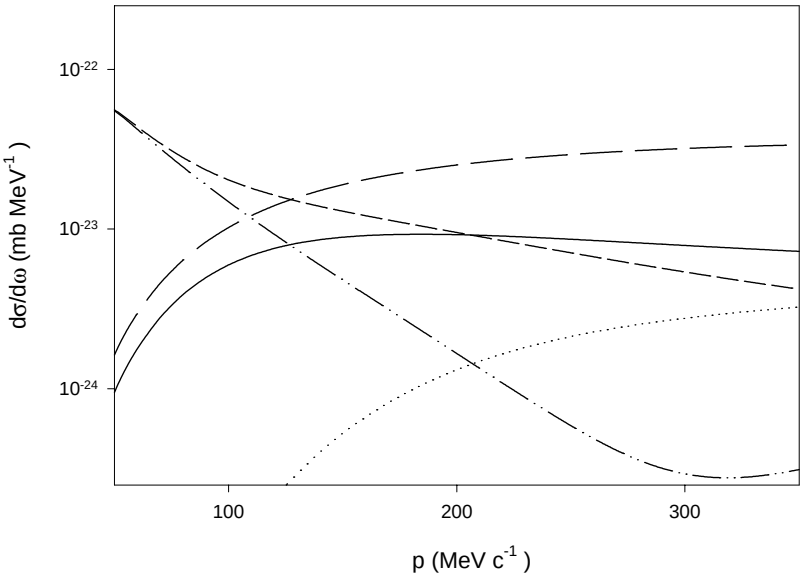

FIG. 2. Cross section $d\sigma/d\omega$ for $n+n\rightarrow n+n+\nu+\bar{\nu}$ as a function of neutron momentum in the c.m. system, for $\omega=1$ MeV, and summed over neutrino flavors. Shown are the result for the OPE (long-dashed curve) and the full T matrix (full curve); in addition, the separate contributions of the T matrix, i.e., $T_{T1}+T_{T2}$ (short-dashed curve), T_{SO} (dotted curve), and T_Q (dashed double-dotted curve) are shown.

Note that in order $k/m \approx p/m$ in the np case there is a nonvanishing contribution for the vector current amplitude. This is analogous to the case of photon bremsstrahlung in NN scattering, where electric-dipole radiation is dominant for the np case. The commutator in Eq. (33) receives contributions from tensor T_{T1} and T_{T2}, quadratic spin-orbit T_Q and spin-orbit T_{SO} components of the direct part of the np T matrix. The anticommutator also receives a central T_C contribution in addition to T_{T1}, T_{T2}, T_Q, and T_{SO} contributions from the exchange part of the np T matrix.

E. Comparison with one-boson exchange (OBE)

In this section we will calculate the neutrino emission cross section in free space. The expression for the cross section in the c.m. system is

$$\frac{d\sigma}{d\omega}=\frac{N_f}{4}\frac{m^3\sqrt{|\vec{p}|^2-\omega E+\omega^2/4}}{6(2\pi)^7(E-\omega/2)|\vec{p}|}\int d\Omega_{\tilde{p}}d^3q(M_\lambda q^\lambda M_\rho^* q^\rho - q^2 M^\lambda M_\lambda^*), \tag{34}$$

which is also given in Timmermans *et al.* [3] with the number of neutrino flavors $N_f=3$. Neutrino pair bremsstrahlung has been calculated mostly, in Born approximation, with a two-nucleon NN interaction consisting of a long range OPE and a phenomenological Landau interaction as shown by Friman and Maxwell [1]. However, the use of lowest order OPE represents a severe approximation. First, it is known that there is a substantial cancellation between the tensor contributions from ρ and pion exchange. Second, it is questionable whether other (momentum dependent) interactions such as the spin-orbit interaction T_{SO} may be ignored. Hanhart *et al.* [2] found that the use of the full T matrix leads to a reduction by a factor 4 compared to OPE for nn bremsstrahlung around saturation density. Our results for nn and np bremsstrahlung is a generalization of Friman and Maxwell's results: The amplitude is computed in terms of the (model independent) on-shell T matrix instead of the Landau plus one-pion exchange interaction in the nonrelativistic limit. The nn phase shifts are, for simplicity, assumed to be equal to the pp phase shifts, which are taken from Ref. [12].

In Fig. 2 the contribution of the various terms of the T matrix, $T_{T1}+T_{T2}$, T_{SO}, and T_Q, to the cross section in the nonrelativistic limit are shown separately for nn bremsstrahlung in free space. The contributions of the quadratic spin-orbit (the T_Q term) and the tensor (the T_{T1} and T_{T2} terms) forces to the cross section cancel at low momenta. The tensor forces (the T_{T1} and T_{T2} terms) dominate over the spin-orbit (the T_{SO} term) and quadratic spin-orbit (the T_Q term) for momenta between 200 MeV/c and 300 MeV/c. From Fig. 2 one may conclude that at larger neutron momentum in the c.m. system, the spin-orbit force (the T_{SO} term) also becomes important.

Several results for the OBE contributions are shown in Fig. 3 for comparison.[1] In the OBE potential contributions considered in this section, the meson-nucleon form factors are not included. They can be neglected because of the relatively small momentum transfer, $|\vec{k}|<2|\vec{p}|$ involved. The OPE result overpredicts the full T-matrix result. At a neutron momentum of $p\approx 300$ MeV/c in the c.m. system, the use of the full T matrix leads to a reduction by a factor of 4–5. Including the tensor part of the one ρ exchange (ORE) to the OPE result is a much better idea. The cancellation of the tensor from OPE at short distance by the tensor from ORE, which has an opposite sign, leads to a result much closer to that obtained with the full T matrix. The result for OPE without the exchange contribution, which is used in most ''standard cooling scenarios,'' is smaller than that for the full OPE, but has a different behavior than the result obtained with the full T matrix. From a neutron momentum of 250 MeV/c in c.m. system, the difference with the result of the full T matrix increases. The contribution from one σ exchange, which gives rise to a spin-orbit force, is also shown to give an estimate of the effect of the other mesons. The effect of the σ is quite small.

[1]Numerical values are taken from the OBE model Nijm93 [13].

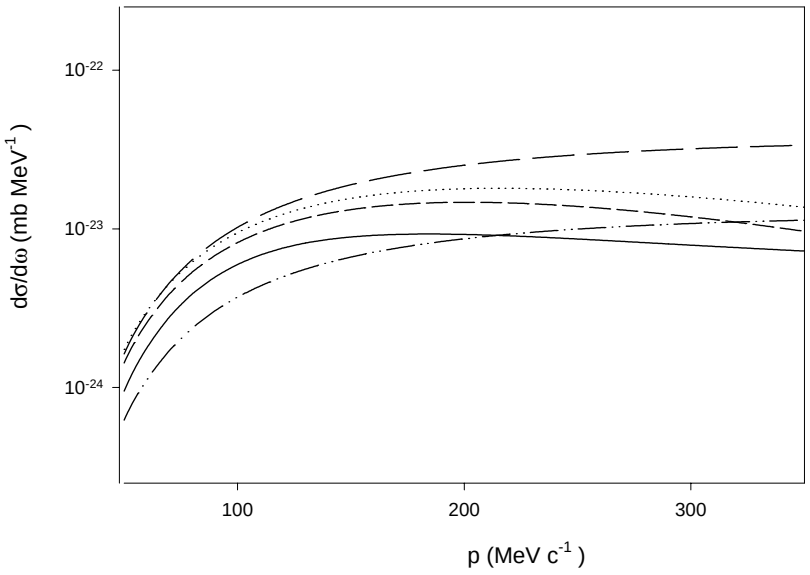

FIG. 3. Cross section $d\sigma/d\omega$ for $n+n\rightarrow n+n+\nu+\bar{\nu}$ as a function of neutron momentum in the c.m. system, for $\omega=1$ MeV, and summed over neutrino flavors. Shown are the results for the OPE (long-dashed curve), one pion+tensor part of ρ exchange (OPtRE) (short-dashed curve), one pion $+\rho+\sigma$ exchange (OPRSE) (dotted curve), OPE without the ''exchange'' contribution (dashed double-dotted curve), and the full T matrix (full curve).

The calculations in Figs. 2 and 3 are done in the nonrelativistic limit. Therefore it is important to check, whether the relativistic corrections are small. We can estimate the importance of the relativistic effects for OPE as well as for the on-shell T matrix taken as the NN interaction.

In Fig. 4 the relative relativistic correction R, in which the magnitude of the relativistic effects are compared to the nonrelativistic cross section, with OPE taken as NN-interaction, is shown. For the $nn\nu\bar{\nu}$ and the $np\nu\bar{\nu}$ processes the nonrelativistic contribution comes from the axial-vector current. The relative relativistic correction R for the $nn\nu\bar{\nu}$ process remains below 15%, and for the $np\nu\bar{\nu}$ process it remains even below 5%. Also in Fig. 4, R is shown for the $nn\nu\bar{\nu}$ process using the T matrix for the NN interaction instead of OPE. The only contributions surviving the nonrelativistic commutator in Eq. (27) come from the T_{T1}, T_{T2}, T_Q, and T_{SO} parts of the T matrix. The relative relativistic correction R for the T matrix remains below 10%. Due to the chosen representation, the spin-spin force is hidden in T_{T1}, T_{T2}, and T_Q. Some components of the on-shell T matrix have a nonrelativistic character (scalar, spin-spin), while others do not (tensor, spin orbit, quadratic spin orbit). In elastic scattering, scalar and spin-spin forces dominate especially at low momenta. In the $nn\nu\bar{\nu}$ process these forces vanish in the nonrelativistic limit of the bremsstrahlung amplitude, because they do not survive the commutator. They still have a nonvanishing relativistic term in the bremsstrahlung amplitude, which explains the increasing importance of the relativistic corrections in the bremsstrahlung amplitude at very low momenta.

III. NEUTRINO EMISSIVITY IN MEDIUM

In this section we consider neutrino bremsstrahlung in a dense hadronic medium at finite temperature. In the simplest

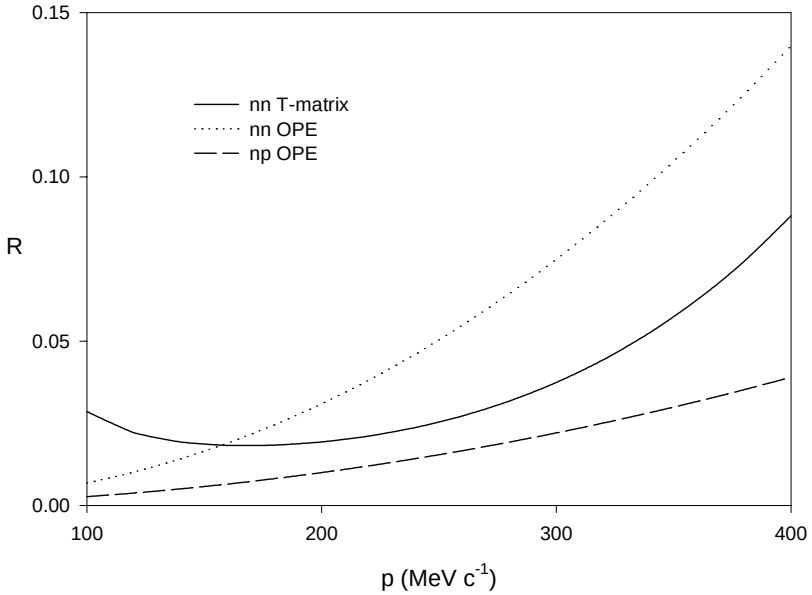

FIG. 4. $R=|\sigma_{NR}-\sigma_R|/\sigma_{NR}$, with σ_{NR} the nonrelativistic cross section and σ_R the cross section, in which also the first-order relativistic corrections are included. Taking the OPE as the NN interaction, the nn and np bremsstrahlung ratios R are given by the dotted curve and the dashed curve, respectively. Also, the nn bremsstrahlung ratio R is shown using the T matrix for the NN interaction.

approach one can use the so-called convolution approximation (followed by Friman and Maxwell [1]) in which the free space bremsstrahlung process is folded with Fermi-Dirac single-particle wave functions and the emission rate is obtained with the use of Fermi's golden rule. This approach is not applicable in more general cases, e.g., if one takes into account dressed propagators. To go beyond the convolution approach, the more general framework of quantum transport theory [14–16] is needed. The latter formalism and the application of the finite temperature Green's functions is summarized in the Appendixes.

A. The emissivity in quantum transport

To compute the emissivity it is convenient to start from the Boltzmann equation (BE) for neutrinos (and antineutrinos), which schematically takes the form (see Appendix A)

$$[\partial_t+\vec{\partial}_q\omega(\vec{q})\vec{\partial}_x]f_\nu(\vec{q},x)\equiv I_\nu^{-+}(\vec{q},x)-I_\nu^{+-}(\vec{q},x), \quad (35)$$

where $f_\nu(\vec{q},x)$ is the single-time distribution function (Wigner function) of the neutrino with $\vec{q}$ the momentum and x being the space-time coordinate. The right hand side (rhs) of Eq. (35) corresponds to the gain and loss collision integral (Appendixes A and B). A similar equation holds for the antineutrinos. For a homogeneous system in Wigner representation, the distribution functions become space independent. Furthermore, the time dependence of the collision integrals can be neglected. Therefore we drop the x argument at the rhs of Eq. (35). The use of the BE provides a general formalism for neutrino and antineutrino emission, absorption, and scattering. The collision integrals I^{-+} and I^{+-} are directly related to the neutrino self-energies Φ^{-+} and Φ^{+-} [Eq. (B2)], which in turn are expressed in terms of the hadronic polarization $S_{\mu\nu}^{-+,+-}(q)$ and the leptonic couplings and propagators [Eq. (B1)]. The former are closely related to retarded polarization or the current-current correlation functions,

$$\begin{aligned} S_{\mu\nu}^{-+}(q)&=S_{\mu\nu}^{+-}(-q)\\ &=2ig_B(\omega)\mathrm{Im}\,\Pi_{\mu\nu}^R(q)\\ &=4\pi i\int d^4\xi\exp(iq\xi)\langle J_\mu^\dagger(0)J_\nu(\xi)\rangle, \end{aligned} \quad (36)$$

with the retarded polarization function $\Pi^R(q)$. The general polarization receives contributions from vector, axial-vector, and interference terms,

$$\Pi_{\mu\nu}(q)=c_V^2\Pi_{\mu\nu}^V(q)+c_A^2\Pi_{\mu\nu}^A(q)+c_Ac_V\Pi_{\mu\nu}^{VA}(q), \quad (37)$$

where $\Pi_{\mu\nu}^V(q)$, $\Pi_{\mu\nu}^A(q)$, and $\Pi_{\mu\nu}^{VA}(q)$ are the vector, the axial-vector, and the mixed parts. In general, one has four independent components $\Pi_{00}^V(q)$, $\Pi_{22}^V(q)$, $\Pi^A(q)$, and $\Pi^{VA}(q)$ [17]. The lepton couplings and propagators give the leptonic tensor $\Lambda^{\mu\nu}=8[q_1^\mu q_2^\nu+q_1^\nu q_2^\mu-(q_1\cdot q_2)g^{\mu,\nu}-i\epsilon^{\alpha\beta\mu\nu}q_{1,\beta}q_{2,\alpha}]$.

In the present case of emission we take the neutrinos to be free. The emissivity (the power of the energy radiated per volume unit) is obtained by multiplying the energy with the left hand side (lhs) of BE (see Appendixes) for neutrinos and antineutrinos, respectively, summing the neutrino and antineutrino expression and integrating over a phase space element:

$$\epsilon_{\nu\bar{\nu}}=\frac{d}{dt}\int\frac{d^3q}{(2\pi)^3}[f_\nu(\vec{q},t)+f_{\bar{\nu}}(\vec{q},t)]\omega(\vec{q}). \quad (38)$$

From Eq. (35) follows

$$\epsilon_{\nu\bar{\nu}}=\int\frac{d^3q}{(2\pi)^3}[I_\nu^{-+,\mathrm{em}}(\vec{q})-I_{\bar{\nu}}^{+-,\mathrm{em}}(\vec{q})]\omega(\vec{q}), \quad (39)$$

where $I_\nu^{-+,\mathrm{em}}(\vec{q})$ and $I_{\bar{\nu}}^{+-,\mathrm{em}}(\vec{q})$ are the terms of the collision integrals, which correspond to the neutrino emission process.

To obtain the emissivity, the leptonic tensor has to be contracted with the structure function

$$\begin{aligned} \epsilon_{\nu\bar{\nu}}=-2\sum_f&\int\frac{d^3q_2}{(2\pi)^3 2\omega(\vec{q}_2)}\int\frac{d^3q_1}{(2\pi)^3 2\omega(\vec{q}_1)}\\ &\times\int\frac{d^4q}{(2\pi)^4}(2\pi)^4\delta^3(\vec{q}_1+\vec{q}_2-\vec{q})\\ &\times\delta[\omega(\vec{q}_1)+\omega(\vec{q}_2)-\omega][\omega(\vec{q}_1)+\omega(\vec{q}_2)]\\ &\times g_B(\omega)\Lambda^{\mu\nu}(q_1,q_2)\mathrm{Im}\,\Pi_{\mu\nu}^R(q). \end{aligned} \quad (40)$$

The number of neutrino flavors is included by the summation over f. For neutrino pair bremsstrahlung, it is more convenient to use in the leptonic tensor $q=q_1+q_2$ instead of q_1 and q_2. Using Lorentz covariance, we can write

$$\begin{aligned} L^{\mu\nu}(q)&=\int\frac{d^3q_1}{\omega_1}\frac{d^3q_2}{\omega_2}\delta^4(q-q_1-q_2)\Lambda^{\mu\nu}(q_1,q_2)\\ &=\frac{8}{3}(q^\mu q^\nu-q^2g^{\mu\nu})\int\frac{d^3q_1}{\omega_1}\frac{d^3q_2}{\omega_2}\delta^4(q-q_1-q_2)\\ &=\frac{16\pi}{3}(q^\mu q^\nu-q^2g^{\mu\nu}). \end{aligned} \quad (41)$$

This simplifies the expression of the emissivity,

$$\epsilon_{\nu\bar{\nu}}=\frac{1}{4(2\pi)^6}\sum_f\int d^4q\,\omega W(q), \quad (42)$$

with $W(q)=-2g_B(\omega)L^{\mu\nu}(q)\mathrm{Im}\,\Pi_{\mu\nu}^R(q)$.

B. Hadronic polarization

Which type of correlation diagrams are dominant in the neutrino-hadron interaction processes depends strongly on the kinematics. In particular, in the spacelike region ($|\vec{q}|>\omega$; scattering), the one-loop QPA diagram and its random phase approximation type iteration dominate; in con-

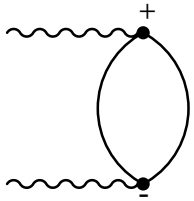

FIG. 5. One-loop contribution to $S^{+-}_{\mu\nu}$.

trast, in the timelike regime ($\omega > |\vec{q}|$), the QPA process is kinematically forbidden and two-body (and many-body) collisions are required as was already clear from the discussion of the free space case.

For practical calculations of the polarization one has to make a choice between the use of dressed Green's functions and the use of quasiparticle Green's functions. On the one hand the use of QPA in the soft limit of $\omega \to 0$ leads to the property that $\mathrm{Im}\,\Pi^R$ behaves as $1/\omega^2$ in all orders, i.e., an infrared divergence (this behavior is correct only for the free case, where the external legs are on-shell ones). Hence one expects that in the soft limit nonperturbative effects play a role (see the LPM effect given below). On the other hand, as pointed out in Ref. [5], in using dressed propagators special care has to be taken to avoid double counting; i.e., one has to restrict oneself to the so-called proper ''skeleton diagrams.'' (An example is the two-loop self-energy insertion in Fig. 6(a), which is already effectively included in the one-loop diagram with full Green's functions.) Another problem connected with the use of dressed Green's functions and bare vertices is the conservation of the vector current.

In general, an expansion in terms of QPA diagrams is simpler (than in terms of full Green's functions) since there are no such spurious diagrams, and also current conservation is satisfied at each loop level. Below we will show that in the special case of an imaginary part of the self-energy (width), there exists a 1-1 correspondence between the QPA and dressed Green's function diagram expansion, i.e., the proper full diagrams can be expressed as multiplicative correction factor $\omega^2/(\omega^2+\Gamma^2)$ to the QPA result. This result allows us to use the QPA and include the finite width at the end.

At low temperatures the leading diagrams are those which contain a minimum number of off-diagonal G^{+-} and G^{-+}. In the closed diagrams the $+-$ and $-+$ lines are cut. In the QPA limit this gives back the original Feynman graphs. The ''$+$'' part is the Feynman amplitude and the ''$-$'' part belongs to the conjugated Feynman amplitude.

1. One loop in QPA

For completeness, we give the one-loop (Fig. 5) polarization function in the QPA limit,

$$iS^{-+}_{\mu\nu}(q) = \int \frac{d^4p}{(2\pi)^4}\frac{d^4p'}{(2\pi)^4}\mathrm{Tr}[\Gamma_\mu G_0^{-+}(p)\Gamma_\nu G_0^{+-}(p')] \times (2\pi)^4\delta^4(q+p'-p), \tag{43}$$

where $\Gamma_\mu = (G_F/2\sqrt{2})\gamma_\mu(c_V - c_A\gamma_5)$.

In the nonrelativistic QPA limit, Eq. (43) can be factorized in terms of a hadronic loop and couplings $X_{\mu\nu}$,

$$\begin{aligned} iS^{-+}_{\mu\nu}(q) &= -2g_B(\omega)\int \frac{d^3p}{(2\pi)^3}\frac{d^3p'}{(2\pi)^3}[f(\epsilon_{\vec{p}}) - f(\epsilon_{\vec{p}'})] \\ &\quad \times (2\pi)^4\delta^4(q+p'-p)X_{\mu\nu} \\ &\equiv 2g_B(\omega)X_{\mu\nu}I_0(q), \end{aligned} \tag{44}$$

with

$$X_{\mu\nu} = \frac{G_F^2}{2}\begin{cases} c_V^2, & \mu=\nu=0 \\ c_A^2, & \mu=\nu=1,2,3. \end{cases} \tag{45}$$

After integration, $I_0(q) = (m^{*2}/2\pi\beta q)\mathcal{L}(q)$, with [17]

$$\begin{aligned} \mathcal{L}(q) = \ln((1+\exp\{-\beta[\epsilon_-(q)-\mu]\})/ \\ (1+\exp\{-\beta[\epsilon_+(q)-\mu]\})), \end{aligned} \tag{46}$$

where $\epsilon_\pm(q) = (\omega^2+\epsilon_{\vec{q}}^2)/4\epsilon_{\vec{q}} \pm \omega/2$, with $\epsilon_{\vec{q}} = \vec{q}^2/(2m^*)$. One sees that in the one-loop approximation in the QPA, only the spacelike contribution ($\omega > |\vec{q}|$) does not vanish.

2. Two loops in QPA

In Fig. 6 the three different types of ''closed diagrams'' at the two-loop level are shown. These diagrams can be considered as (lowest order) propagator, vertex, and interaction renormalization of the one loop in QPA, respectively. We begin considering the simple case of nn neutrino pair bremsstrahlung with the on-shell T matrix in Eq. (11). Figure 6(a) contains terms with the acausal propagator G^{++} and the causal propagator G^{--} with the same arguments, which can be $p_i - q$ or $p_i' + q$, whereas Fig. 6(b) contains terms with a G^{++} and G^{--} with different arguments (opposite signs for q), and one obtains for Figs. 6(a) and 6(b),

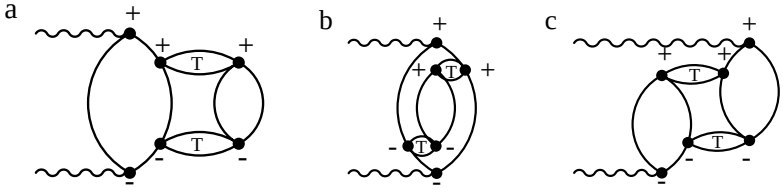

FIG. 6. The three different types of ''closed diagrams'' at the two-loop level. These diagrams can be considered as (a) (lowest order) propagator, (b) vertex, and (c) interaction renormalization of the QPA.

$$
\begin{aligned}
&i[S^{-+,(a)}_{\mu\nu}(q)+S^{-+,(b)}_{\mu\nu}(q)]\\
&\quad=\sum_{\alpha=1}^{5}\sum_{\beta=1}^{5}\int\left[\prod_{i=1}^{2}\frac{d^4p_i}{(2\pi)^4}\frac{d^4p_i'}{(2\pi)^4}\right]\\
&\qquad\times\frac{d^4k}{(2\pi)^4}T^1_\alpha T^1_\beta{}^*(\mathrm{Tr}[\Omega^{--}_\beta G_0^{-+}(p_2)\Omega^{++}_\alpha G_0^{+-}(p_2')]\\
&\qquad\times\mathrm{Tr}[\Delta^{--}_{\alpha,\mu,1}G_0^{-+}(p_1)\Delta^{++}_{\alpha,\nu,1}G_0^{+-}(p_1')]\\
&\qquad+\{1\leftrightarrow2\})(2\pi)^8\delta^4(k+p_2'-p_2)\delta^4(q+p_1'-k-p_1),
\end{aligned}
\tag{47}
$$

with $\Delta^{++}_{\alpha,\mu,i}=\Omega^{++}_\alpha G_0^{++}(p_i-q)\Gamma_\mu+\Gamma_\mu G_0^{++}(p_i'+q)\Omega^{++}_\alpha$, $\Delta^{--}=(\Delta^{++})^*$, and $\Gamma_\mu=(G_F/2\sqrt{2})\gamma_\mu(c_V-c_A\gamma_5)$. The definition of Ω^{++} is given in Eq. (12) and Ω^{--} follows from the relation $\Omega^{--}=\gamma_0\Omega^{++}\gamma_0$. Thus in the nonrelativistic limit, Figs. 6(a) and 6(b) have opposite signs $\pm1/\omega$. One obtains for Fig. 6(c),

$$
\begin{aligned}
iS^{-+,(c)}_{\mu\nu}=&\int\sum_{\alpha=1}^{5}\sum_{\beta=1}^{5}\left[\prod_{i=1}^{2}\frac{d^4p_i}{(2\pi)^4}\frac{d^4p_i'}{(2\pi)^4}\right]\frac{d^4k}{(2\pi)^4}\\
&\times T^1_\alpha T^1_\beta{}^*(\mathrm{Tr}[\Delta^{--}_{\alpha,\nu,2}G_0^{-+}(p_2)\Omega^{++}_\alpha G_0^{+-}(p_2')]\\
&\times\mathrm{Tr}[\Omega^{--,\beta}G_0^{-+}(p_1)\Delta^{++}_{\alpha,\nu,1}G_0^{+-}(p_1')]+\{1\leftrightarrow2\})\\
&\times(2\pi)^8\delta^4(k+p_2'-p_2)\delta^4(q+p_1'-k-p_1).
\end{aligned}
\tag{48}
$$

Note that only the $-+$ and $+-$ lines are cut in the diagrams of Fig. 6, since cutting the T matrix would lead to double counting.

The above expressions become simpler if the QPA Green's functions are used [see Eqs. (C7)–(C9)],

$$
\begin{aligned}
iS^{-+}_{\mu\nu}(q)=&\sum_{\alpha=1}^{5}\sum_{\beta=1}^{5}\int\frac{d^4k}{(2\pi)^4}\left[\prod_{i=1}^{2}\frac{d^3p_i}{(2\pi)^3}\frac{d^3p_i'}{(2\pi)^3}\right.\\
&\left.\times f(\tilde{E}_i)[1-f(\tilde{E}_i')]\right](2\pi)^8\delta^4(k+p_2'-p_2)\\
&\times\delta^4(q+p_1'-k-p_1)X_{\mu\nu},
\end{aligned}
\tag{49}
$$

where X contains all operators and $f(\tilde{E}_i)=\{\exp[\beta(\tilde{E}_i-\mu)]+1\}^{-1}$ with $\tilde{E}$ the relativistic energy and μ the relativistic chemical potential. In particular, for Figs. 6(a) and 6(b), we obtain

$$
\begin{aligned}
X^{(a)}_{\mu\nu}+X^{(b)}_{\mu\nu}=&\sum_{\alpha=1}^{5}\sum_{\beta=1}^{5}T^1_\alpha T^1_\beta{}^*(\mathrm{Tr}[\Omega^{++,\alpha}\Lambda^+(p_2^*)\Omega^{--,\beta}\\
&\times\Lambda^+(p'^*_2)]\mathrm{Tr}[\Delta^{++}_{\alpha,\mu,1}\Lambda^+(p_1^*)\Delta^{--}_{\beta,\nu,1}\Lambda^+(p'^*_1)]\\
&+\{1\leftrightarrow2\}),
\end{aligned}
\tag{50}
$$

and for Fig. 6(c), we obtain

$$
\begin{aligned}
X^{(c)}_{\mu\nu}=&\sum_{\alpha=1}^{5}\sum_{\beta=1}^{5}T^1_\alpha T^1_\beta{}^*(\mathrm{Tr}[\Delta^{++,\alpha}_{\mu,2}\Lambda^+(p_2^*)\Omega^{--,\beta}\Lambda^+(p'^*_2)]\\
&\times\mathrm{Tr}[\Omega^{++}_\alpha\Lambda^+(p_1^*)\Delta^{--}_{\beta,\nu,1}\Lambda^+(p'^*_1)]+\{1\leftrightarrow2\}).
\end{aligned}
\tag{51}
$$

One verifies that the sum of all two-loop diagrams conserves the vector current, i.e., $q^\mu S^{-+}_{\mu\nu}(q)=0$. First, Fig. 6(c) is current conserving on its own. That the sum of Figs. 6(a) and 6(b) is current conserving can easily be deduced from Eq. (20) by noting that $q^\mu[p_\mu/(p_i\cdot q)-p'_{i\mu}/(p_i'\cdot q)])=0$. In the following, the hadronic part of interaction matrix $X_{\mu\nu}$ is evaluated in the nonrelativistic limit for the cases A,V,VA, separately.

C. The nonrelativistic limit

Although in principle X can be evaluated relativistically, we will use the simpler nonrelativistic formalism. First we consider the vector current $X^V_{\mu\nu}$. Expanding the Green's functions G^{++} and G^{--} (see Appendix C) in powers of $(\vec{p}\cdot\vec{q})/(m^*\omega)$ leads to

$$
X^{(a),V}_{\mu\nu}+X^{(b),V}_{\mu\nu}+X^{(c),V}_{\mu\nu}=\frac{c_V^2G_F^2}{8}V_\mu V_\nu|T^{nn}|^2+O(|\vec{p}|^3/m^{*3}),
\tag{52}
$$

where

$$
\begin{aligned}
V_\mu=\frac{1}{m^*\omega}\Bigg[&-p_{1\mu}\left(1+\frac{\vec{p}_1\cdot\vec{q}}{m^*\omega}\right)+p'_{1\mu}\left(1+\frac{\vec{p}'_1\cdot\vec{q}}{m^*\omega}\right)\\
&+\{1\leftrightarrow2\}\Bigg]
\end{aligned}
\tag{53}
$$

and

$$
|T^{nn}|^2=4(|T_C|^2+|T_Q|^2+|T_{T1}|^2+|T_{T2}|^2+2|T_{SO}|^2).
\tag{54}
$$

We see that in leading order in the nonrelativistic limit, with $G^{++}(p\pm q)\Gamma_\mu\rightarrow\pm p_\mu/(m^*\omega)$, the vector contributions cancel due to $p'_{1\mu}+p_{2\mu}-p'_{1\mu}-p'_{2\mu}\approx0$, while the separate diagrams do not vanish.

For the axial-vector current to obtain the nonrelativistic limit we expand the G^{--} and G^{++} functions in powers of $(\vec{p}\cdot\vec{q})/(m^*\omega)$, and replace the coupling $\Gamma^A_\mu\rightarrow\vec{\sigma}\cdot\vec{p}/m^*\ \delta_{\mu,0}+\sigma_i\delta_{\mu,i}$. For Figs. 6(a) and 6(b), the hadronic part of the interaction matrix is

$$
X^{(a),A}_{00}+X^{(b),A}_{00}\approx O(|\vec{p}|^2/m^{*2}),
\tag{55}
$$

$$X_{ij}^{(a),A}+X_{ij}^{(b),A}=\frac{c_A^2G_F^2}{8\omega^2}\sum_{v=2}^{5}8|\mathcal{T}_v|^2\Bigg[\mathrm{Tr}[(\vec{\sigma}_1\times\vec{l}_v)^i(\vec{\sigma}_1\times\vec{l}_v)^j]\times\left(1+\frac{(\vec{p}_1+\vec{p}_1')\cdot\vec{q}}{m^*\omega}+O(|\vec{p}|^2/m^{*2})\right)+\{1\leftrightarrow2\}\Bigg] \tag{56}$$

and

$$X_{0j}^{(a),A}+X_{0j}^{(b),A}=\frac{c_A^2G_F^2}{8\omega^2}\sum_{v=2}^{5}8|\mathcal{T}_v|^2(\mathrm{Tr}[(\vec{\sigma}_1\times\vec{l}_v)^j\times(\vec{\sigma}_1\times\vec{l}_v)\cdot(\vec{p}_1+\vec{p}\,'_1)]+O(|\vec{p}|^2/m^{*2})+\{1\leftrightarrow2\}) \tag{57}$$

with

$$\vec{l}_v=(\vec{l}_1,\vec{l}_2,\vec{l}_3,\vec{l}_4,\vec{l}_5)=(\vec{n},\vec{n},\vec{k},\vec{k}',\vec{n}). \tag{58}$$

Hence in leading order in the nonrelativistic limit there is a contribution to the axial-vector current (the contribution from the central interactions to the axial-vector current vanishes, since they commute with the weak spin operator). For Fig. 6(c), one has

$$X_{00}^{(c),A}\approx O(|\vec{p}|^2/m^{*2}), \tag{59}$$

$$X_{ij}^{(c),A}=\frac{c_A^2G_F^2}{8\omega^2}\sum_{v=2}^{4}\sum_{u=2}^{4}16(\mathcal{T}_v^1\mathcal{T}_u^{1*}+\mathcal{T}_u^1\mathcal{T}_v^{1*})\times(\vec{l}_v\times\vec{l}_u)^i(\vec{l}_u\times\vec{l}_v)^j\left(1+\frac{(\vec{p}_1+\vec{p}\,'_1+\vec{p}_2+\vec{p}\,'_2).\vec{q}}{m^*\omega}+O(|\vec{p}|^2/m^{*2})\right), \tag{60}$$

$$X_{0j}^{(c),A}=\frac{c_A^2G_F^2}{8\omega^2}\sum_{v=2}^{4}\sum_{u=2}^{4}16(\mathcal{T}_v^1\mathcal{T}_u^{1*}+\mathcal{T}_u^1\mathcal{T}_v^{1*})\times(\vec{l}_v\times\vec{l}_u)^j\{\vec{l}_v\cdot[(\vec{p}_1+\vec{p}_2+\vec{p}\,'_1+\vec{p}\,'_2)\times\vec{l}_u]\}+O(|\vec{p}|^2/m^{*2}), \tag{61}$$

with $i=j=1,2,3$. The definitions for $\mathcal{T}$ are given in Eq. (18).

As for the mixed VA contribution in the nonrelativistic limit, the traces vanish, and hence

$$X^{(a),VA}+X^{(b),VA}+X^{(c),VA}\approx O(p^2/m^{*2}). \tag{62}$$

Therefore, we obtain the (well-known) result [1] that in leading order in the nonrelativistic limit there is only a nonvanishing contribution from the axial-vector current. In free space, Fig. 4 shows that at momenta relevant at nuclear matter densities the p/m corrections to neutrino pair emission are only of the order of 10%. Therefore, one may conclude that the leading order nonrelativistic result with only the axial-vector current constitutes a good approximation. Contracting the polarization function $S_{\mu\nu}^{-+}(q)$ with the leptonic tensor $L^{\mu\nu}(q)=(16\pi/3)(q^\mu q^\lambda-q^2g^{\mu\lambda})$ yields

$$W(q)=i\mathrm{Tr}[L^{\mu\nu}(q)(S_{\mu\nu}^{-+,(a)}(q)+S_{\mu\nu}^{-+,(b)}(q)+S_{\mu\nu}^{-+,(c)}(q))]=\frac{2\pi g_A^2G_F^2}{3\omega^2}\int\prod_{i=1}^{2}\left[\frac{d^3p_i}{(2\pi)^3}\frac{d^3p_i'}{(2\pi)^3}f(E_i)[1-f(E_i)]\right]\times|M|^2\delta^4(q+p_1'+p_2'-p_1-p_2), \tag{63}$$

where

$$|M|^2=32\sum_{v=2}^{5}|\mathcal{T}_v^1|^2[(2\omega^2-|\vec{q}|^2)|\vec{l}_v|^2-(\vec{q}\cdot\vec{l}_v)^2]+16\sum_{v=2}^{4}\sum_{u=2}^{4}(\mathcal{T}_v^1\mathcal{T}_u^{1*}+\mathcal{T}_v^{1*}\mathcal{T}_u^1)[((\vec{l}_v\times\vec{l}_u)\cdot\vec{q})^2+(\vec{l}_v\times\vec{l}_u)^2(\omega^2-|\vec{q}|^2)]. \tag{64}$$

D. The LPM effect

The free space NN neutrino-pair bremsstrahlung process exhibits an infrared $1/\omega$ divergence (see Sec. II C). The QPA result in Eq. (63) also shows an infrared divergence, reminiscent of the free space bremsstrahlung. It is well known that the singularity in the electromagnetic bremsstrahlung process is suppressed in a medium, the Landau-Pomeranchuk-Migdal (LPM) effect, whenever the mean free path of the emitting particle becomes comparable to the photon formation length, $\omega-\vec{v}\cdot\vec{q}$. The former is characterized by the imaginary part of the self-energy, Γ, of the emitting particle, while the photon formation length can be approximated in the nonrelativistic limit by the formation energy, ω. Therefore, the LPM effect is expected to become effective whenever $\omega\approx\Gamma$.

The LPM effect has been discussed recently in various contexts. For instance, for photon emission in a quark gluon plasma by Aurenche *et al.* [18] and Cleymans *et al.* [19] in terms of thermal field theory. Analogously, one expects similar effects in the electroweak case (as noted by Raffelt [20] for neutrino pair and axion production in supernovas and neutron stars).

Here we estimate the LPM effect on the response function S and the emissivity as a function of the temperature and density by using the dressed propagators for G^{-+}, G^{+-}, and G^{--} in Eqs. (C11)–(C13). Note that in a fully dressed Green's function formalism the diagram of Fig. 6(a) is not a proper skeleton diagram and its contribution is already included in the fully dressed one-loop diagram. In this case the appropriate irreducible diagrams to be considered are given by the dressed one loop, the corresponding two-loop vertex correction (these together conserve already the vector current) and the two-loop interaction normalization. We evaluate these in the limit of $\Gamma=2\,\mathrm{Im}\,\Sigma<\mathrm{Re}\,\Sigma$. Following Ref. [5] we note that in the limit $\Gamma=\mathrm{const}$ and $q\to0$, it is possible

to write the fully dressed diagrams in terms of the lowest nonvanishing order in the QPA in the low temperature limit. A remark has to be made about the one-loop result,

$$iS^{-+}(q) \approx \frac{m^* p_F \omega}{\pi^2} \frac{\Gamma}{\omega^2 + \Gamma^2}. \tag{65}$$

We note that it is possible to relate the one-loop result to the lowest nonvanishing order in the QPA, if the quasiparticle width Γ in the numerator is represented by the one-loop QPA self-energy

$$\Gamma = \mathrm{Im} \quad . \tag{66}$$

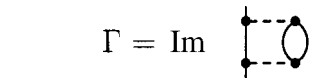

In the low temperature limit one can make the approximations $f(E_{p'}+\omega) \approx 0$ and $f(E_p - \omega) \approx 1$, which lead to

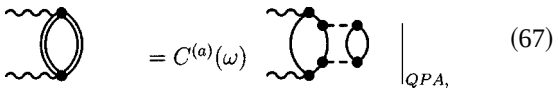

$$= C^{(a)}(\omega) \Big|_{QPA,} \tag{67}$$

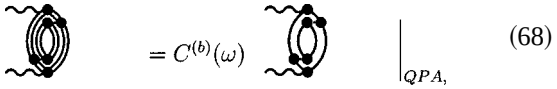

$$= C^{(b)}(\omega) \Big|_{QPA,} \tag{68}$$

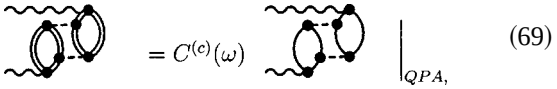

$$= C^{(c)}(\omega) \Big|_{QPA,} \tag{69}$$

where $C^{(a)}(\omega) = C^{(b)}(\omega) = C^{(c)}(\omega) = \omega^2/(\omega^2 + \Gamma^2)$.

We note that with the present $C^{(b)}$ [which differs from the result given in Ref. [5], namely, $C^{(b)} = [\omega^2(\omega^2 - \Gamma^2)]/(\omega^2 + \Gamma^2)^2$] the conserved vector current relation holds, because the vector current is conserved in the QPA limit.

If only the dressed off-shell propagators G^{++} and G^{--} are kept while G^{+-} is replaced by G_0^{+-}, we find a different result for the damping, $\tilde{C} = \omega^2/(\omega^2 + \Gamma^2/4)$. From this we conclude that the dressing of all G's should be considered on equal footing. In some previous works (e.g., Raffelt and Seckel [20]), the quasiparticle width has been included directly (in a rather *ad hoc* fashion) in the cross section by replacing $1/\omega^2$ by a modified one, $1/(\omega^2 + a^2\Gamma^2)$, where a is taken to be unity. In this case Γ is purely a parameter with no microscopic origin; in reality, Γ depends on momentum, density, and temperature.

E. Modification of the *T* matrix in the medium

Above, we have considered the T matrix in free space. In the past, the possible medium modification of the T matrix has been addressed only in a very few papers. The Rostock group has studied the effect of the medium on neutrino emissivities [21] in the framework of a thermal dynamic T matrix. It was found that at $T = 4$ MeV, the ratio R of emissivities for the in-medium T matrix to the free T-matrix result is about 0.8 for nuclear saturation density for the modified URCA process, and a striking ≈ 0.05 for the neutral current bremsstrahlung process. The latter effect was ascribed to the Pauli blocking of the low momentum states. The results were obtained using a separable approximation to the potential neglecting $^3P_2$-$^3F_2$ tensor coupling. Here we estimate the medium effect by using a G matrix at zero temperature to account for Pauli blocking, which includes the full tensor force. The Bethe-Goldstone equation for the G matrix is

$$G(\vec{p}', \vec{p}) = V(\vec{p}', \vec{p}) + \sum_{\lambda, i} \int \frac{d^3p''}{(2\pi)^3} V(\vec{p}', \vec{p}'') \frac{Q_{Pauli}}{E(\vec{p}'') - \epsilon(\vec{p})} G(\vec{p}'', \vec{p}), \tag{70}$$

where λ, i are the helicities and isospin of the intermediate state, respectively. The single-nucleon energy above and below the Fermi momentum p_F are $E(\vec{p})$ and $\epsilon(\vec{p})$, respectively. Here the G matrix of Banerjee and Tjon [22] in the lowest order Brueckner theory (LOBT) is used; the single-nucleon energies are given by

$$E(\vec{p}) = \frac{\vec{p}^2}{2m}, \quad \epsilon(p) = A + \frac{\vec{p}^2}{2m^*}.$$

The gap A and the effective mass m^* are determined in the LOBT in a self-consistent way. As an interaction in Eq. (70), the Bonn C potential is used, and for Q_{Pauli} in Eq. (70) an angle averaged Pauli operator is used to construct the G matrix.

IV. RESULTS AND DISCUSSION

We will compare the emissivity of the nn neutrino pair bremsstrahlung for the different NN interactions at densities $n = 1/2n_0$, n_0, and $2n_0$ at $T = 10^9$ K. We will derive the expression of the emissivity in the nonrelativistic QPA limit starting from Eq. (42). From Eqs. (63) and (64) the function $W(q)$ is obtained. Here, the momentum $\vec{q}$ is neglected in the momentum conserving δ function, because it is much smaller than the neutron momenta. Next we separate the angular and energy parts of the nucleon phase space by performing the angular integrals with the momenta of the degenerate neutrons approximated by the neutron Fermi momenta. Finally, we use the independence of the matrix elements of $\vec{q}$ and introduce the dimensionless parameter $y = \omega/T$ to simplify the expression, and one obtains

$$\epsilon_{\nu,\bar{\nu}} = \frac{4G_F^2 g_A^2 m^{*4} p_{Fn}}{15(2\pi)^9} T^8 \int dy d\cos(\theta_{12}) d\cos(\theta_{11'}) \frac{H(s,t)}{\sqrt{2 + 2\cos\theta_{12}}} I(y), \tag{71}$$

where

$$I(y) = \frac{(4\pi^2 y^5 + y^7)}{6[1 + \exp(y)]} \tag{72}$$

and the hadronic part of the interaction matrix

TABLE I. Emissivity in 10^{19} erg cm^{-2} s^{-1} at $T=10^9$ K.

	Neutron matter			Symmetric matter		
Density	$(1/2)n_0$	n_0	$2n_0$	$(1/2)n_0$	n_0	$2n_0$
m^*/m	0.77	0.64	0.49	0.66	0.58	0.49
OPE	7.3	4.8	2.1	2.7	2.4	1.6
OPRE	3.9	2.3	1.0	1.7	1.3	0.8
OPROE	3.2	2.0	0.9	1.4	1.0	0.7
OBE	3.7	2.5	1.3	1.5	1.2	0.9
OPE+TPE	10.2	6.9	3.7	3.5	3.2	2.3
OPRE+TPRE	4.4	2.8	1.4	1.8	1.4	1.0
OPROE+TPROE	1.2	1.2	2.7	0.4	0.3	0.4
OBE+TBE	1.4	0.6	0.3	0.8	0.5	0.2
T matrix	2.2	1.1		1.1	0.7	0.4
R matrix	2.5	1.4		1.2	0.8	0.5
G matrix	2.7	1.6	0.6	1.2	0.9	0.5

$$H(s,t)=\left(8\sum_{v=1}^{5}|\mathcal{T}_v^1|^2+2\sum_{v=2}^{4}\sum_{v\neq u;u=2}^{4}(\mathcal{T}_v^1\mathcal{T}_u^{1*}+\mathcal{T}_v^{1*}\mathcal{T}_u^1)\right) \tag{73}$$

is a function of the Mandelstam variables s,t and p_{Fn} is the neutron Fermi momentum. The integration variable θ_{12} is the angle between $\vec{p}_1$ and $\vec{p}_2$, and $\theta_{11'}$ is the angle between $\vec{p}_1$ and $\vec{p}_1'$. We note that in the limit that the G matrix is replaced by the antisymmetrized one-pion (or one-ρ) exchange potential, Eq. (71) reduces to the result of Friman and Maxwell [1].

The results for the emissivities are summarized in Table I for neutron matter for three different densities, $n=1/2n_0$, n_0, and $2n_0$ at $T=10^9$ K. It is seen that (similarly, as in free space) compared to the T matrix result the antisymmetrized OPE overestimates the emission rate by roughly a factor of 4; this is in agreement with the conclusion by Hanhart *et al.* [2]. If the exchange terms in OPE are (arbitrarily) omitted, the result is close to that of the T matrix. In the past, in some cases phenomelogical correction factors are also introduced to simulate initial and final state interactions as a correction to OPE [1,23], which tend to reduce the OPE result. Contrary to naive expectations, based on the Pauli blocking mechanism we find a slight increase in the rate if the T matrix is replaced by the in-medium G matrix as calculated by the Bethe-Goldstone equation described in the preceding section.

To obtain more insight in the medium effects we also listed in the table the separate results for one-pion, pion+ ρ, pion+ρ+ω (OPROE), and full OBE (which includes also σ exchange), and also for the corresponding OBE plus iterated OBE (i.e, OBE+ TBE). It is seen that one-ρ exchange gives a substantial cancellation of the OPE (also observed by Friman and Maxwell [1]). On the other hand, the iterated OPE (referred to as TPE) leads to a stronger tensor force, and hence a larger rate. It is also seen that the contributions of ω exchange and σ exchange (which contribute mainly to the spin-orbit interactions) are non-negligible, in particular, in the TBE process; and as a consequence, the combined OBE and TBE contribution becomes even smaller than the full T matrix result. These momentum dependent interactions do not appear in the conventional Landau–Fermi liquid interaction, but do seem to play a role in the weak bremsstrahlung. We attribute the finding that the G matrix gives a slightly larger contribution than the free T matrix mainly to a Pauli blocking of the TBE contributions, and hence a smaller destructive interference. We note that the present result deviates from that in Ref. [21] where at $n=n_0$ in neutron matter the ratio of the rates computed with G matrix and T matrix was found to be 0.05; a possible explanation could be the neglect of the $^3P_2$-$^3F_2$ tensor coupling in that work.

As to the density dependence the decrease of the rate with increasing density is mainly caused by the variation of m^* in Eq. (71) and to a lesser extent by the different ranges of the various meson exchanges. For completeness we also show the corresponding results for symmetric nuclear matter in Table I. The weaker density dependence in this case can be attributed to less variation of m^*.

Finally, we turn to the LPM effect. Clearly, its possible relevance in the present case depends on the magnitude of the width Γ, which is a function of ω, temperature T, and density. Here we use the parametrization [6]

$$\Gamma(\omega,T)=a\left(\frac{\omega^2}{4\pi^2}+T^2\right) \tag{74}$$

to be able to estimate the importance of the LPM effect. For $\omega<60$ MeV and $T<20$ MeV, this roughly coincides within a factor 2 with Alm *et al.* [24]. Including the LPM effect in the emissivity the function $I(y)$ in Eq. (71) has to be replaced by

$$I_{LPM}(y,T)=y^2f(y,T)I(y) \tag{75}$$

with

$$f(y,T)=1\Big/\left(y^2+\frac{\Gamma(yT,T)^2}{T^2}\right),$$

which can be derived from Eqs. (67)–(69). The function $f(y,T)$ describes very roughly the behavior of $\mathrm{Im}\,\Pi^R$. To give an indication of the importance of the LPM effect and to demonstrate the influence of the weighting factor in the emissivity, we show in Fig. 7 how the functions $f(y,T)$ and $I_{LPM}(y,T)$ in Eq. (75) are modified for various values of the temperature. The value of the parameter a depends weakly on the density and is ≈ 0.2 MeV c^{-1}. One sees that the function $f(y,T)$ has a singularity at $y=0$ in the QPA. The LPM effect suppresses this infrared divergence. The function $I_{LPM}(y,T)$ is less sensitive to the LPM effect compared to the function $f(y,T)$, because the weighting factor in the emissivity strongly suppresses the $y=0$ contribution. Therefore, the LPM effect in the emissivity is negligible for $T<5$ MeV. Comparing the ratio of the emissivity with and without LPM effect $R_{LPM}=\epsilon/\epsilon_{lpm}$ at $T=5$ MeV, $T=10$ MeV, and $T=20$ MeV gives 0.89, 0.68, and 0.35, respectively. The influence of the LPM effect increases with temperature and becomes appreciable above $T=5$ MeV. There-

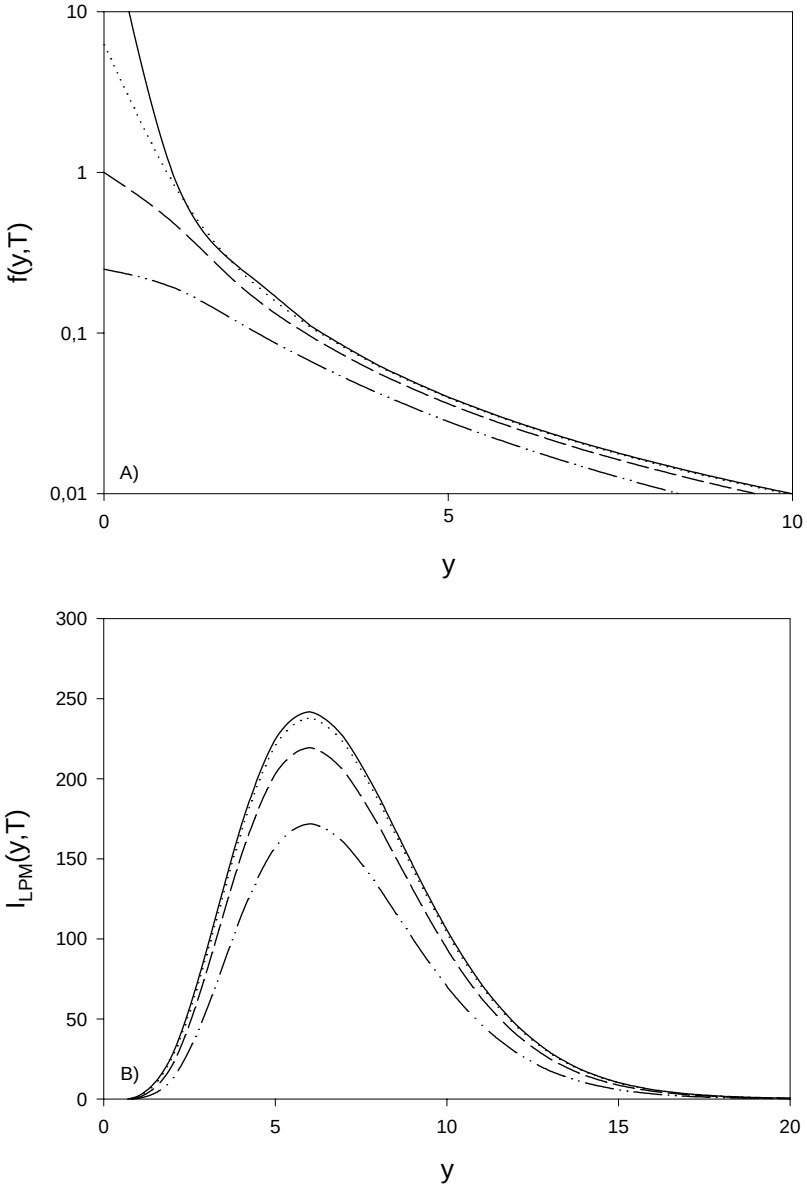

FIG. 7. The functions $f(y,T)$ and $I_{LPM}(y,T)$ are shown at temperature $T=2$ MeV (dotted curve), $T=5$ Mev (dashed curve), and $T=10$ MeV (dash-dotted curve). The QPA result is given by the solid line.

fore, in practice in calculating the emissivity the LPM effect does not play an important role for small T, say $T<5$ MeV.

Finally, we note that an additional medium effect, not considered here, is the possible medium effect of the axial-vector coupling g_A. It has been considered in Ref. [25], where it was found that the spacelike axial coupling is quenched by about 20%. However, the timelike axial coupling is not necessarily equal, since Lorentz invariance is broken. Experiments with first-forbidden β decay of light nuclei give indications for an enhancement of the timelike axial charge of about 25% in the medium [26]. This is in agreement with meson exchange calculations in the soft pion approximations [27].

V. SUMMARY AND CONCLUSION

In this paper we studied the neutrino emissivity for the neutral current NN bremsstrahlung process, relevant for neutron star cooling. In particular, we considered some effects that are not included in the standard cooling scenario of Ref. [1], which is based upon a nonrelativistic quasiparticle approximation and the use of the one-pion exchange potential. The effects considered, namely, the description of the NN interaction, the LPM effect, and relativistic effects, influence the neutrino emission of the neutral current bremsstrahlung process. Therefore these effects are also expected to affect other neutrino emission processes in a similar way.

First, we studied how the description of the NN interaction influences the NN bremsstrahlung process. In the low density limit using the fact that ω is small, the Low theorem [9] can be applied, which allows us to use the on-shell T matrix, specified by empirical phase shifts, and to compare it with OPE. At typical neutron momenta in neutron stars, approximately 300 MeV/c, the resulting free space cross section is roughly a factor 4–5 reduced compared to the application of OPE. Although adding ORE to OPE is an improvement, the result still differs a factor 2–3 with that obtained using the T matrix. We also analyzed which Fermi

components of the T matrix dominate the rate, namely, the tensor-type and the spin-orbit-type terms.

To evaluate neutrino-pair bremsstrahlung in a finite medium at finite temperature, we have used a closed diagram technique up to two loops. It is found that at $n \sim n_0$, the neutrino emissivity, applying the on-shell T matrix to describe the NN interaction is roughly a factor 4 smaller than those based upon OPE. This is in qualitative agreement with the conclusion of Hanhart [2]. Including medium effects from Pauli blocking by replacing the T matrix by an in-medium G matrix,we find a small increase of the emissivity of 20–30 %.

Second, in order to investigate the many-body correlations, we can go beyond QPA by considering dressed propagators with a temperature dependent imaginary part Γ. Of course gauge invariance of the vector current is conserved in our approach. In particular, we find that in the medium the damping of the infrared divergence, the LPM effect, has a negligible effect for low temperatures ($T < 5$ MeV); this is due to both the small single-particle width ($\Gamma \approx T^2$) and a weighting factor depending on ω in the phase space integral. Finally, we estimated relativistic (recoil) effects to be rather small, of the order of 10%, at nuclear saturation densities.

In short, the description of the NN interaction by the on-shell T matrix OPE has the largest impact on the neutrino emission of the bremsstrahlung process; roughly a reduction factor of 4. Other effects are relatively small; below 30% percent for $T < 5$ MeV.

ACKNOWLEDGMENTS

This work had been supported through the Stichting voor Fundamenteel Onderzoek der Materie with financial support from the Nederlandse Organisatie voor Wetenschappelijk Onderzoek. The work of J.A.T. was supported by the U.S. Department of Energy Contract No. DE-AC05-84ER40150, under which the Southeastern Universities Research Association (SURA) operates the Thomas Jefferson National Accelerator Facility. We thank R. G. E. Timmermans and S. Reddy for helpful discussions.

APPENDIX A: NEUTRINO TRANSPORT

In the present paper we use the finite temperature real time Schwinger-Keldysh formalism to compute the collision integrals in the transport formalism. For the sake of completeness, the main steps are summarized in this appendix; for more details we refer to Ref. [6]. In this formalism one must distinguish between vertices with indices $(+)$ and $(-)$. For given real interaction, these are associated with the value $-iV$ (time-ordered part) and with adjoint vertex $+iV$ (anti-time-ordered part). The corresponding finite temperature Green's functions (applied to neutrinos as well as the nucleons) can be expressed as a 2×2 matrix propagator:

$$i\underline{G}_{1,2} = \begin{pmatrix} G_{12}^{--} & G_{12}^{-+} \\ G_{12}^{+-} & G_{12}^{++} \end{pmatrix} = \begin{pmatrix} \langle T\psi(x_1)\overline{\psi}(x_2)\rangle & -\langle \overline{\psi}(x_2)\psi(x_1)\rangle \\ \langle \psi(x_1)\overline{\psi}(x_2)\rangle & \langle \tilde{T}\psi(x_1)\overline{\psi}(x_2)\rangle \end{pmatrix}. \quad \text{(A1)}$$

Sometimes it is more convenient to use the retarded and advanced functions:

$$iG_{12}^{R} = \theta(t_1 - t_2)\langle\{\psi(x_1), \overline{\psi}(x_2)\}\rangle,$$
$$iG_{12}^{A} = \theta(t_1 - t_2)\langle\{\psi(x_1), \overline{\psi}(x_2)\}\rangle. \quad \text{(A2)}$$

The propagators satisfy the Dyson equation,

$$\underline{G}(x_1,x_2) = \underline{G}_0(x_1,x_2) + \underline{G}_0(x_1,x_3)\underline{\Phi}(x_3,x_2)\underline{G}(x_2,x_1), \quad \text{(A3)}$$

where $\underline{\Phi}$ is the proper self-energy. Equivalently, in integro-differential form,

$$\not{\partial}_1 \underline{G}_{1,2} = \delta_{1,2}\underline{\sigma_z} + \underline{\sigma_z}\int d3\,\underline{\Phi}_{13}\underline{G}_{3,2}, \quad \text{(A4)}$$

$$\not{\partial}_2^{*} \underline{G}_{1,2} = \delta_{1,2}\underline{\sigma_z} + \int d3\,\underline{G}_{1,3}\underline{\Phi}_{3,2}\sigma_z, \quad \text{(A5)}$$

where σ_z is the Pauli spin matrix. The semiclassical neutrino transport equations are obtained by subtracting the Dyson equations (A4) and (A5) for ∂_1 and ∂_2,

$$i\underline{G}(x_1,x_2)\not{\partial}_{x_2} - i\not{\partial}_{x_1}\underline{G}(x_1,x_2) = \underline{G}(x_1,x_3)\underline{\Phi}(x_3,x_2)\underline{\sigma_z} - \underline{\sigma_z}\,\underline{\Phi}(x_1,x_3)\underline{G}(x_3,x_2). \quad \text{(A6)}$$

In particular, the transport equation for the off-diagonal matrix Green's function reads

$$[\not{\partial}_{x_3} - \mathrm{Re}\,\Phi^R(x_1,x_3), G^{+-,-+}(x_3,x_2)] - [\mathrm{Re}\,G^R(x_1,x_2), \Phi^{+-,-+}(x_3,x_2)] = \frac{1}{2}\{G^{+-,-+}(x_1,x_3), \Phi^{+-,-+}(x_3,x_2)\} + \frac{1}{2}\{\Phi^{+-,-+}(x_1,x_2), G^{+-,-+}(x_3,x_2)\}. \quad \text{(A7)}$$

As a result of the assumption of the existence of the Lehmann representation, we have $\mathrm{Re}\,G^R = \mathrm{Re}\,G^A = \mathrm{Re}\,G$ and $\mathrm{Re}\,\Phi^R = \mathrm{Re}\,\Phi^A = \mathrm{Re}\,\Phi$. The Wigner transforms of the off-diagonal Green's functions correspond to Wigner densities in four-coordinate and four-momentum space. In the gradient expansion the Wigner transforms of convolution integrals can be expressed in terms of Poisson brackets (PB) $\{A,B\}_{PB} = \partial_k A \partial_x B - \partial_x A \partial_k B$. This leads to the quasiclassical neutrino transport equation in which the neutrino self-energies enter in the loss and gain terms,

$$i\{\mathrm{Re}\,G^{-1}(p,x), G^{+-,-+}(p,x)\}_{PB} + i\{\mathrm{Re}\,G(p,x), \Phi^{+-,-+}(p,x)\}_{PB} = G^{+-,-+}(p,x)\Phi^{+-,-+}(p,x) + \Phi^{+-,-+}(p,x)G^{+-,-+}(p,x). \quad \text{(A8)}$$

The first Poisson bracket at the lhs leads (Vlasov part) to the Boltzmann drift term, whereas the second one corresponds to off-mass shell effects. After separating the pole and nonpole terms:

$$G^{+-,-+}(p,x)=G_0^{+-,-+}(p,x)+G_{\rm off}^{+-,-+}(p,x),$$

the quasiparticle part of the transport equation is given by

$$\begin{aligned} i\{\mathrm{Re}\ G^{-1}(p,x),G_0^{+-,-+}(p,x)\}_{PB} \\ =G^{+-,-+}(p,x)\Phi^{+-,-+}(p,x) \\ -\Phi^{+-,-+}(p,x)G^{+-,-+}(p,x), \end{aligned} \tag{A9}$$

where $\mathrm{Re}\,G^{-1}(p,x)=\not{p}-\mathrm{Re}\,\Phi^R(p,x)$. The lhs corresponds to the drift term of the Boltzmann equation and the rhs to the collision integrals. The remainder part of the transport equation,

$$\begin{aligned} i\{\mathrm{Re}\ G^{-1}(p,x)G_{off}^{+-,-+}(p,x)\}_{PB} \\ +i\{\mathrm{Re}\ G(p,x),\Phi^{+-,-+}(p,x)\}_{PB}=0, \end{aligned} \tag{A10}$$

describes the off-shell effects, which we neglect.

The on-mass-shell neutrino propagator is related to the single-time distribution functions (Wigner functions) of neutrinos and antineutrinos, $f_\nu(q)$ and $f_{\bar\nu}(q)$,

$$\begin{aligned} G_0^{-+}(q,x)=\frac{i\pi\not{q}}{\omega(\vec q)}\{\delta[q_0-\omega(\vec q)]f_\nu(q,x)-\delta[q_0+\omega(\vec q)] \\ \times[1-f_{\bar\nu}(-q,x)]\}, \end{aligned} \tag{A11}$$

and in the G_0^{+-} propagator $f_\nu(q)$ is replaced by $1-f_\nu(q)$ and $1-f_{\bar\nu}(q)$ by $1-f_{\bar\nu}(q)$. In this limit the Boltzmann equation for the neutrino distributions is obtained,

$$\begin{aligned} [\partial_t+\vec\partial_q\,\omega(\vec q)\vec\partial_x]f_\nu(\vec q,x) \\ =\int_0^\infty\frac{dq_0}{2\pi}\mathrm{Tr}[\Phi^{-+}(q,x)G_0^{+-}(q,x) \\ -\Phi^{+-}(q,x)G_0^{-+}(q,x)] \\ \equiv I_\nu^{-+}(\vec q,x)-I_\nu^{+-}(\vec q,x), \end{aligned} \tag{A12}$$

where the rhs corresponds to the gain and loss term (the Boltzmann equation for antineutrino follows by integration over the negative q_0).

APPENDIX B: COLLISION INTEGRALS

In the lowest (second) order in the weak interaction, the neutrino transport self-energies are given by

$$\begin{aligned} -i\Phi^{-+,+-}(q,x)=\int\frac{d^4q_1}{(2\pi)^4}\frac{d^4q_2}{(2\pi)^4}(2\pi)^4\delta^4(q_1+q_2-q) \\ \times i\Gamma_{q_1}^{\mu}iG_0^{-+}(q_2,x)i\Gamma_{q_1}^{\dagger\lambda}iS_{\mu\lambda}^{-+,+-}(q_1,x), \end{aligned} \tag{B1}$$

where $S_{\mu\lambda}^{-+,+-}(q)$ is the baryon polarization tensor and Γ_q^μ is the weak leptonic interaction vertex.

The collision integrals in Eq. (A12), which are expressed as a convolution of the lepton self-energies Φ and the intermediate (anti)neutrino propagator, consist of a sum of a loss and a gain term; e.g., the neutrino gain part

$$I_\nu^{-+}(\vec q,x)=\int_0^\infty\frac{dq_0}{2\pi}\mathrm{Tr}[\Phi^{-+}(q,x)G_0^{+-}(q,x)] \tag{B2}$$

contains a (spacelike) scattering [proportional to $f_\nu(1-f_\nu)$] and a (timelike) pair emission term [$\propto(1-f_{\bar\nu})(1-f_\nu)$]. The antineutrino one is obtained by replacing the positive energy range by the negative one.

APPENDIX C: FINITE *T* HADRONIC GREEN'S FUNCTIONS

Although in the neutrino sector the stationary condition $\Phi^{-+}G_\nu^{+-}=\Phi^{+-}G_\nu^{-+}$ is not satisfied (see Appendix B), in the hadronic sector it is. Therefore the nucleons can be treated in the equilibrium Green's function formalism. The retarded self-energy Σ^R can be decomposed in Lorentz components, in nuclear matter only the scalar and vector components are nonzero,

$$\Sigma^R(p)=\Sigma_S^R(p)+\not{\Sigma}_V^R(p)$$

with $p=(p^0,\vec p)$. The retarded relativistic dressed baryon Green's function [15] is

$$G^R(p)=\frac{\not{p}+m-\not{\Sigma}_V^R(p)+\Sigma_S^R(p)}{[p-\Sigma_V^R(p)][p-\Sigma_V^R(p)]-[m+\Sigma_S^R(p)]^2}, \tag{C1}$$

and the spectral function

$$A(p)=-2\ \mathrm{Im}\ G^R(p). \tag{C2}$$

Using Eqs. (C1) and (C2) we can now give the following relations:

$$G^{-+}(p)=if(p^0)A(p), \tag{C3}$$

$$G^{+-}(p)=-i[1-f(p^0)]A(p), \tag{C4}$$

$$G^{--}(p)=[1-f(p^0)]G^R(p)+f(p^0)G^A(p), \tag{C5}$$

$$G^{++}(p)=-[1-f(p^0)]G^A(p)-f(p^0)G^R(p), \tag{C6}$$

with $f(p_0)=1/\{\exp[\beta(p^0-\mu)]+1\}$, $\beta=1/kT$, and the chemical potential $\mu=E_{p_F}+\mathrm{Re}\,\Sigma_V^{0,R}(p_F)$. We will now define the relativistic effective Dirac mass $m_D=m+\mathrm{Re}\,\Sigma_S^R(p)$,

$\tilde{p}^0 = p^0 - \mathrm{Re}\,\Sigma_V^{0,R}(p)$, $\vec{\tilde{p}} = \vec{p} + \mathrm{Re}\,\vec{\Sigma}_V^R(p)$, $\tilde{E}_p = \sqrt{(\vec{\tilde{p}})^2 + (m_D)^2}$, and $\Gamma = 2\mathrm{Im}[-\Sigma_V^{0,R} - (m_D/\tilde{E}_p)\Sigma_S^R(p) + (\vec{\tilde{p}}/\tilde{E}_p)\vec{\Sigma}_V^R(p)]$. We will consider two cases, (i) the QPA Green's functions $\mathrm{Im}\,\Sigma(p) \to 0$ and (ii) the nonrelativistic Green's functions.

1. Green's functions in QPA

In the QPA case, the imaginary part of self-energy $\mathrm{Im}\Sigma(p)$ vanishes. This gives the following definitions for the Green's functions in Eqs. (C3)–(C6),

$$G_0^{+-}(p) = -2i\pi \frac{m_D \Lambda^+(\tilde{p})}{\tilde{p}^0}[1 - f(p^0)]\delta(\tilde{p}^0 - \tilde{E}_p), \tag{C7}$$

$$G_0^{-+}(p) = 2i\pi \frac{m_D \Lambda^+(\tilde{p})}{\tilde{p}^0} f(p^0)\,\delta(\tilde{p}^0 - \tilde{E}_p), \tag{C8}$$

$$G_0^{--}(p) = [G_0^{++}(p)]^* = \frac{2m_D \Lambda^+(\tilde{p})}{\tilde{p}^2 - m_D^2}, \tag{C9}$$

where we have the positive-energy operator $\Lambda^+(\tilde{p}) = (\tilde{\not{p}} + m_D)/2m_D$. The causal propagators G_0^{--} and G_0^{++} are off-mass-shall. If $\tilde{p}$ is on-mass-shell $\tilde{p}^2 - m_D^2 = 0$, then G^{--} can be rewritten as

$$G_0^{--}(p \pm q) = [G_0^{++}(p \pm q)]^* = \frac{2m_D \Lambda^+(\tilde{p})}{\pm 2\tilde{p}\cdot q}. \tag{C10}$$

We point out that, when taking complex conjugates, it is understood that Dirac γ matrices are not conjugated. The free case can easily be obtained from this. By replacing m_D, $\tilde{p}$ by m and p, we obtain the free Green's functions.

2. The nonrelativistic Green's functions

In this part will be given the nonrelativistic Green's functions. Besides the nonrelativistic limit, we will assume that the width of the quasiparticle state is small, $\mathrm{Im}\,\Sigma^R(p) \ll \mathrm{Re}\,\Sigma^R(p)$. We will now define the Green's functions in the nonrelativistic limit as

$$G^{-+}(p) = \frac{i\Gamma(p)}{(p^0 - \eta_{\vec{p}})^2 + \Gamma(p)^2/4} f(p^0), \tag{C11}$$

$$G^{+-}(p) = \frac{-i\Gamma(p)}{(p^0 - \eta_{\vec{p}})^2 + \Gamma(p)^2/4}[1 - f(p^0)], \tag{C12}$$

and

$$G^{--}(p) = [G^{++}(p)]^* = \frac{p^0 - \eta_p}{[p^0 - \eta_{\vec{p}}]^2 + \Gamma(p)^2/4} - \frac{i\Gamma(p)}{[p^0 - \eta_{\vec{p}}]^2 + \Gamma(p)^2/4}\tanh\left(\frac{p^0}{2}\right), \tag{C13}$$

where $\Gamma(p) = -2\,\mathrm{Im}[\Sigma_V^{0,R}(p) + \Sigma_S^R(p)]$, $\tanh(p^0) = 1 - 2f(2p^0)$, and $\eta_{\vec{p}} = \epsilon_{\vec{p}}^0$ with $\epsilon_{\vec{p}}^0 = |\vec{p}|^2/(2m^*)$ and m^* the nonrelativistic effective mass.

[1] B.L. Friman and O.V. Maxwell, Astrophys. J. **232**, 541 (1979).
[2] C. Hanhart, D.R. Philips, and S. Reddy, Phys. Lett. B **499**, 9 (2001).
[3] R. Timmermans, A.Yu. Korchin, E.N.E. van Dalen, and A.E.L. Dieperink, Phys. Rev. C **65**, 064007 (2002).
[4] D.N. Voskresensky and A.V. Senatorov, Zh. Eksp. Teor. Fiz. **90**, 1505 (1986) [Sov. Phys. JETP **63**, 885 (1986)].
[5] J. Knoll and D.N. Voskresensky, Ann. Phys. (N.Y.) **249**, 532 (1996).
[6] A. Sedrakian and A.E.L. Dieperink, Phys. Rev. D **62**, 083002 (2000).
[7] M.E. Gusakov, Astron. Astrophys. **389**, 702 (2002).
[8] D.G. Yakovlev, A.D. Kaminker, P. Haensel, and O.Y. Gnedin, Astron. Astrophys. **389**, L24 (2002).
[9] F.E. Low, Phys. Rev. **110**, 974 (1958).
[10] M.L. Goldberger, M.T. Grisaru, S.W. MacDowell, and D.Y. Wong, Phys. Rev. **120**, 2250 (1960); M.L. Goldberger, Y. Nambu, and R. Oehme, Ann. Phys. (N.Y.) **2**, 726 (1957).
[11] J.A. Tjon and S.J. Wallace, Phys. Rev. C **32**, 267 (1985).
[12] V.G.J. Stoks, R.A.M. Klomp, M.C.M. Rentmeester, and J.J. de Swart, Phys. Rev. C **48**, 792 (1993).
[13] V.G.J. Stoks, R.A.M. Klomp, C.P.F. Terheggen, and J.J. de Swart, Phys. Rev. C **49**, 2950 (1994).
[14] W. Botermans and R. Malfliet, Phys. Rep. **198**, 115 (1990).
[15] J.E. Davis and R.J. Perry, Phys. Rev. C **43**, 1893 (1991).
[16] F. de Jong and R. Malfliet, Phys. Rev. C **44**, 998 (1991).
[17] S. Reddy, M. Prakash, J.M. Lattimer, and J.A. Pons, Phys. Rev. C **59**, 2888 (1999).
[18] P. Aurenche, F. Gelis, and H. Zaraket, Phys. Rev. D **62**, 096012 (2000).
[19] J. Cleymans, V.V. Goloviznin, and K. Redlich, Phys. Rev. D **47**, 989 (1993).
[20] G. Raffelt and D. Seckel, Phys. Rev. D **52**, 1780 (1995).
[21] D. Blaschke, G. Röpke, H. Schulz, A.D. Sedrakian, and D.N. Voskresensky, Mon. Not. R. Astron. Soc. **273**, 596 (1995).
[22] M.K. Banerjee and J.A. Tjon, Nucl. Phys. **A708**, 303 (2002) .
[23] D.G. Yakovlev, A.D. Kaminker, O.Y. Gnedin, and P. Haensel, Phys. Rep. **354**, 1 (2001).
[24] T. Alm, G. Röpke, A. Schnell, N.H. Kwong, and H.S. Köhler, Phys. Rev. C **53**, 2181 (1996).
[25] G.W. Carter and M. Prakash, Phys. Lett. B **525**, 249 (2002).
[26] E.K. Warburton, I.S. Towner, and B.A. Brown, Phys. Rev. C **49**, 824 (1994).
[27] I.S. Towner, Nucl. Phys. **A542**, 631 (1992).